BMC Nephrology

RESEARCH Open Access

Novel insights into the molecular mechanisms of sepsis-associated acute kidney injury: an integrative study of GBP2, PSMB8, PSMB9 genes and immune microenvironment characteristics

Haiting Ye[1,2], Xiang Zhang[4], Pengyan Li[1], Mei Wang[2], Ruolan Liu[2] and Dingping Yang[1,3*]

Abstract

Background Sepsis-associated acute kidney injury (SA-AKI) is a prevalent and severe complication of sepsis, but its complex pathogenesis remains unclear. This study aims to identify potential biomarkers for SA-AKI by elucidating its molecular mechanisms through bioinformatics methods.

Methods Transcriptional data related to SA-AKI were obtained from the Gene Expression Omnibus (GEO) database. We used differentially expressed genes (DEGs) and weighted gene co-expression network analysis (WGCNA) to identify characteristic genes associated with SA-AKI and conducted enrichment analyses. Hub genes were determined using protein-protein interaction (PPI) network analysis and the Least Absolute Shrinkage and Selection Operator (LASSO). Additionally, ROC curves were plotted to assess the diagnostic value of these core genes. Immune cell infiltration was analyzed using the CIBERSORT algorithm, and potential associations between the hub genes and clinicopathological features were explored based on the Nephroseq database. Finally, a murine model of SA-AKI was induced with lipopolysaccharide (LPS) to validate the findings, and mRNA abundance and protein production levels of pivotal genes were confirmed via RT-qPCR, Western blotting, and immunohistochemical methods.

Results We identified 268 characteristic genes associated with SA-AKI that are enriched in immune and inflammation-related pathways. Utilizing machine learning techniques, three key genes were screened: *GBP2, PSMB8* and *PSMB9*. The expression patterns of these three genes were well-validated through animal experiments and databases. Correlation between these genes and clinical indicators was confirmed using the Nephroseq database. Furthermore, immune infiltration analysis provided additional insights into their potential functions.

Conclusion *GBP2, PSMB8*, and *PSMB9* are promising candidate genes for SA-AKI, providing a novel perspective on its pathological mechanisms. Further exploration of the biological roles of these genes in the pathogenesis of SA-AKI is needed in the future.

*Correspondence:
Dingping Yang
shenbinneike@163.com

Full list of author information is available at the end of the article

Keywords Sepsis-associated acute kidney injury, Bioinformatics, LASSO, WGCNA, Immune infiltration

Introduction

SA-AKI constitutes a sophisticated microcirculatory dysfunction that entails a considerable risk of advancing to chronic kidney disease (CKD) and renal failure, ultimately giving rise to notable morbidity and mortality burdens. Recent clinical statistics reveal that the incidence of SA-AKI in intensive care units increased from 14% in 2015 to 18% in 2021, with a mortality rate reaching 18% [1]. Additionally, patients with SA-AKI exhibit a markedly greater demand for renal replacement therapy compared to those with non-sepsis-induced AKI, underscoring the severity and therapeutic challenges posed by SA-AKI [2]. Given its substantial clinical burden—including high morbidity, mortality, and long-term adverse outcomes leading to chronic kidney dysfunction that affects socioeconomic factors—SA-AKI has emerged as a pressing public health issue globally [3]. Thus, exploring the potential molecular mechanisms underlying SA-AKI is essential for developing more precise diagnostic methods, identifying valuable molecular biomarkers, effectively monitoring disease progression, accurately assessing prognosis, and discovering potential therapeutic intervention targets.

The pathogenic mechanisms of SA-AKI primarily involve dysregulated inflammatory responses, microcirculatory dysfunction, and cellular metabolic reprogramming [4]. First, sepsis-induced microvascular alterations are characterized by decreased capillary density and an increase in both non-flowing and intermittently flowing capillaries, leading to a reduced surface area for substance exchange. This results in inadequate oxygen and nutrient delivery to the kidneys, impairing metabolic waste removal and contributing to SA-AKI [5]. Second, during the pathogenesis of sepsis, specific molecules bind to receptors located on the surface of target renal tubular epithelial cells, subsequently triggering a series of intracellular signaling pathways. This leads to an upregulation of inflammatory cytokines, which aids the body in combating and clearing invading bacteria [6]. However, the activation of these inflammatory mediators exacerbates oxidative stress and mitochondrial damage, accelerating the progression of SA-AKI [7]. Furthermore, in response to inflammatory signals, the metabolic pathways of monocytes and T cells undergo a shift during the acute phase, transitioning from a reliance on oxidative phosphorylation (OXPH) to enhanced aerobic glycolysis. This shift promotes the differentiation of these immune cells into phenotypes with greater pro-inflammatory activity. Subsequently, inflammatory cells revert to OXPHOS and restore anti-inflammatory phenotypes, facilitating organ function recovery [8]. In summary, the intricate interplay among dysfunctional microcirculation, deregulated inflammatory responses, and reprogrammed cellular metabolic patterns creates a complex pathological network, rendering the pathogenesis of SA-AKI complex and elusive.

In recent years, the discipline of bioinformatics has seen remarkable achievements, with numerous tools being continuously developed and widely applied in disease diagnosis, targeted drug development, and other areas [9, 10]. In investigating disease models of SA-AKI, to more accurately mimic human disease states, several studies have employed omics analyses using peripheral blood samples from sepsis patients [11, 12]. However, it is noteworthy that the analytical results from peripheral blood samples do not fully encapsulate the pathological changes of SA-AKI at the renal tissue level. Clinically, obtaining renal tissue samples from AKI patients with sepsis alone is extremely challenging, making mouse models indispensable in SA-AKI research. In SA-AKI mouse models established using cecal ligation and puncture technology, Liu et al.'s study revealed the functional roles of ferroptosis and m6A RNA methylation regulators in SA-AKI based on transcriptome data and PPI network analysis [13]. Li et al.'s research, leveraging proteomics data combined with DEG analysis and a comprehensive review of existing literature, identified aldose reductase AKR1B1 as a critical player in the pathogenesis of SA-AKI [14]. To effectively exclude the interference of other potential factors such as tissue injury repair, Xu et al.'s study used LPS to induce an SA-AKI mouse model, combining proteomics with metabolomics to comprehensively analyze the multidimensional characteristics of SA-AKI from a macroscopic perspective, with particular emphasis on the importance of sepsis-induced renal mitochondrial dysfunction and metabolic disorders during SA-AKI [15]. Omics technologies enable the comprehensive detection of all relevant biological information in a specific sample, generating vast amounts of data. By leveraging various bioinformatics tools, disease models can be analyzed from multiple perspectives, yielding diverse results [16]. However, these analytical outcomes necessitate robust validation for support. Therefore, in this study, we analyzed renal tissue data from LPS-AKI mice from a transcriptomics perspective, combining forward validation through animal experiments with reverse validation using datasets from other disease models. This approach enhanced the reliability of our analytical findings.

In this study, we selected the transcriptomics datasets GSE240304 related to SA-AKI as our training set. Through differential expression analysis and WGCNA,

we identified characteristic genes closely associated with SA-AKI and explored their biological functions through enrichment analysis. Furthermore, we employed the maximum clique centrality (MCC) and Degree algorithms on the Cytoscape platform, along with LASSO regression analysis, to identify three critical hub genes for SA-AKI: *GBP2, PSMB8*, and *PSMB9*. To further understand the immune cell infiltration in SA-AKI, we performed analysis using the CIBERSORT tool. In addition, we evaluated diagnostic efficacy of these key genes and their potential correlations with clinicopathological characteristics. Finally, to validate the expression patterns of these genes, we performed RT-qPCR, Western blot analysis, and immunohistochemical staining in a mouse model of AKI induced by LPS. The workflow chart is illustrated in Fig. 1.

Methods

Data collection

We used the keywords "sepsis" and "AKI" to search for datasets related to SA-AKI in the GEO database (https://www.ncbi.nlm.nih.gov/geo/). After screening, we selected five datasets, GSE240304 (https://www.ncbi.nlm.nih.gov/gge/download/?acc=GSE240304%26format=file%26file=GSE240304%5FmRNA%5FExpression%5FSummary%2Etxt%2Egz), GSE30718 (https://www.ncbi.nlm.nih.gov/geo/download/?acc=GSE30718%26format=file), GSE268009 (https://www.ncbi.nlm.nih.gov/geo/query/acc.cgi?acc=GSE268009), GSE106993 (https://www.ncbi.nlm.nih.gov/geo/query/acc.cgi?acc=GSE106993), GSE130795 (https://www.ncbi.nlm.nih.gov/geo/query/acc.cgi?acc=GSE130795), GSE199598 (https://www.ncbi.nlm.nih.gov/geo/query/acc.cgi?acc=GSE199598) and GSE30576 (https://www.ncbi.nlm.nih.gov/geo/query/acc.cgi?acc=GSE30576) for further study. Among them, GSE240304 served as the training set, focusing on mouse renal tissue with 5 normal control samples, 5 LPS-induced AKI samples, and 5 cisplatin-induced AKI samples, while the remaining datasets were utilized as validation sets. GSE30718 encompasses 28 samples of acute kidney injury (AKI), 11 stable renal transplant samples, and 8 normal biopsy control samples. GSE268009 consists of renal tissue samples from 6 control mice and 6 mice with ischemia-reperfusion injury-induced AKI (IRI-AKI). GSE106993 includes renal tissue samples from 4 control mice and 4 mice with cisplatin-induced AKI. GSE130795 contains renal tissue samples from 3 control mice and 3 mice with contrast-induced AKI. GSE199598 comprises 4 control mice and 4 mice in the LPS-AKI group, where mice received an LPS injection dose of 5 mg/kg. In GSE30576, mice were

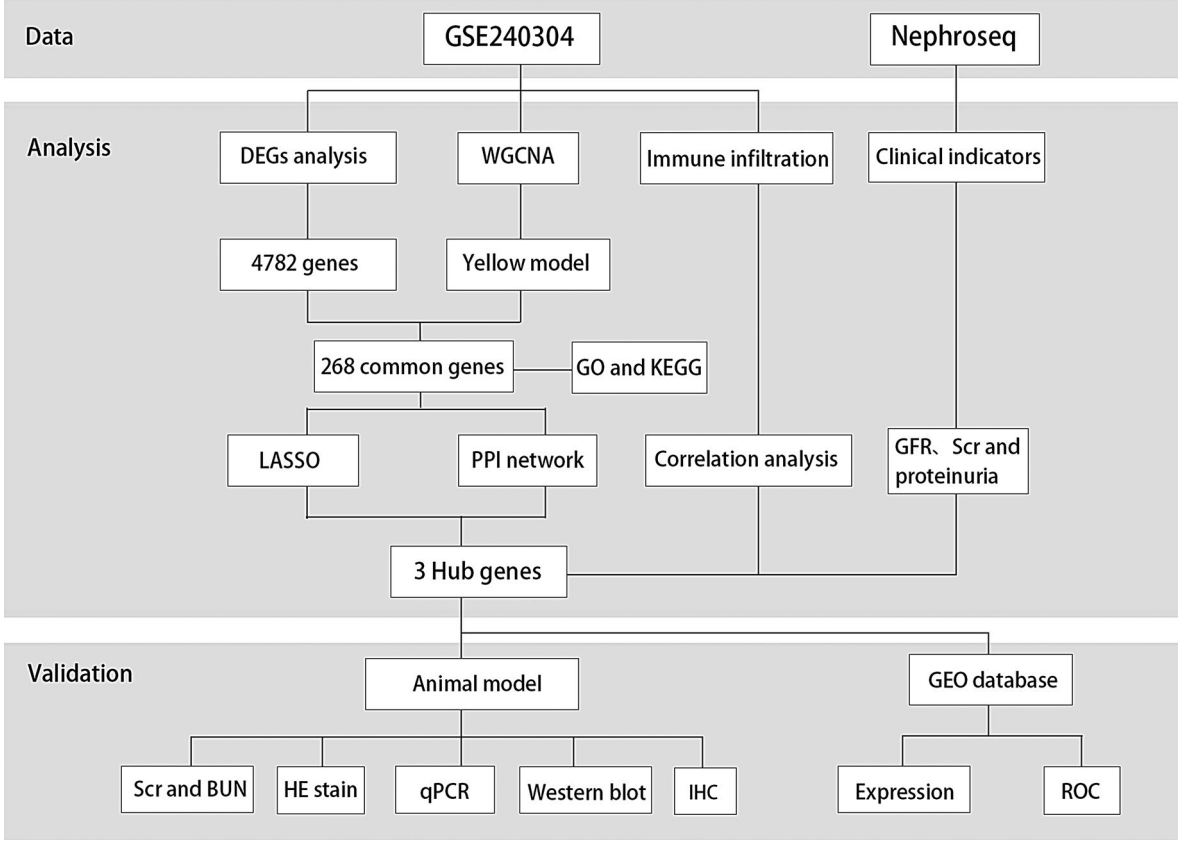

Fig. 1 Design and analysis process of the study

divided into four groups of three each after receiving an LPS injection of 10 mg/kg. The baseline group was assessed at 0 hours post-LPS injection, the early renal injury group at 18 hours post-injection, the renal function recovery group was treated with saline at 18 hours and assessed at 42 hours (with most mice recovering from AKI), and the persistent renal injury group, which did not recover, was also assessed at 42 hours. The microarray dataset platform and series matrix files were saved in text format. During data analysis, R software (version 4.3.1) was employed to match probe names with gene names, taking the average when several probes targeted the identical gene.

Gene differential expression analysis

In order to compare the differences in gene expression between the SA-AKI group and the normal control group, we utilized the "limma" package in R as our analytical tool and established the following screening criteria: the adjusted p-value needed to be less than 0.05 (corrected using the Benjamini & Hochberg method), and the absolute value of the logarithm of the fold change in gene expression (|log(FC)|) needed to be greater than 1.

Weighted gene co-expression network analysis

As is commonly known, WGCNA is an analytical tool designed to construct networks by identifying co-expression patterns among genes, and further explore the potential associations between these network modules and specific biological phenotypes [17]. In this study, we used the "WGCNA" package in R to analyze the GSE240304 dataset. identifying and removing outlier samples, we merged highly correlated modules with a clustering height limit of 0.25. We set a minimum of 30 genes module. The optimal soft threshold (β) was determined when the scale-free topology model fit index was 0.9 ($R^2 = 0.9$). Sequently, modules were merged based on their association with the disease. The optimal module was selected for further analysis, and the relationship between the gene module and SA-AKI was explored by analyzing the values of gene significance (GS) and module membership (MM).

Enrichment analysis of characteristic genes

Gene Ontology (GO) is an important ontology in the field of bioinformatics that provides a standardized vocabulary for describing the molecular function (MF), cellular component (CC), biological processes (BP) of genes and their products [18]. The Kyoto Encyclopedia of Genes and Genomes (KEGG) is a comprehensive bioinformatics database that integrates biological pathways, chemicals, enzymes, genes, and proteins, primarily used to identify significantly related biological pathways for gene sets [19]. We carried out GO and KEGG enrichment analyses on SA-AKI-linked characteristic genes to delve into their biological functions and pathways, employing the DAVID bioinformatics tool (https://davidbioinformatics.nih.gov) [20], setting a significance threshold of $p < 0.05$. Char acteristic genes of SA-AKI were identified using a Venn diagram (https://jvenn.toulouse.inrae.fr/app/index.html).

Identification of hub genes in the PPI network

The STRING database (http://string-db.org/) integrates PPI data from multiple sources. Based on this database, we constructed a PPI network for the characteristic genes of SA-AKI. To ensure the reliability of the network, we set a medium confidence level (0.4) as the minimum scoring criterion for interactions. To improve the connectivity of the network, we removed all disconnected network nodes [21]. Each node represents a unique protein, while connections between nodes indicate molecular interactions. We utilized CytoHubba plugin of Cytoscape software (version 3.7.0) to compute the Degree and MCC values for each intersection, reflecting connectivity and centrality within the network [22]. The fifteen genes with the highest rankings were chosen for additional analysis.

Identification of hub genes by LASSO analysis

LASSO analysis is a statistical method for variable selection and regularization that constructs a penalty function to create a simpler model. By adjusting parameters, LASSO effectively controls model sparsity and prevents overfitting, allowing for the selection of significant variables from a large set [23]. In this study, we performed LASSO regression analysis on SA-AKI characteristic genes.

Hub gene selection and diagnostic value assessment

The intersection of the results from Degree, MCC, and LASSO identified the hub genes for SA-AKI. Based on the GSE3078 dataset, we validated the differential expression of these hub genes. Meanwhile, corresponding ROC curves were plotted and the area under the curve (AUC) was calculated. Genes with an AUC value exceeding 0.5 were considered to have significant clinical value. Furthermore, we have downloaded three datasets: IRI-AKI, Cis-AKI, and CI-AKI, for the initial assessment of the disease specificity of the core genes. Concurrently, we downloaded two datasets of LPS-AKI with different doses to investigate whether the severity of infection influences the diagnostic value of the core genes.

Immune cell infiltration analysis

CIBERSORT was utilized to quantitatively analyze the percentages of different immune cell subtypes in individual sample. A histogram was generated to illustrate the infiltration of 25 immune cell types across different

samples [24]. Additionally, a violin plot was created to visually compare immune cell differences between SA-AKI and normal tissues. Finally, we conducted a Spearman correlation analysis to explore the potential correlations between significant genes and immune cells.

Correlation of hub genes with clinicopathological features

We explored the correlation between SA-AKI hub genes and glomerular filtration rate, serum creatinine, and proteinuria using the Nephroseq database (https://nephroseq.org/).

Animal experiments

LPS-AKI animal model

Twelve male C57BL/6 mice were acquired from the Animal Experiment Center at Renmin Hospital of Wuhan University. They were aged between 6 and 8 weeks and weighed between 20 and 22 grams. Using a random number table, mice were randomly assigned to two groups: control (Control) and model (LPS), with 6 mice per group. In the model group, LPS (Servicebio, Wuhan, China) was administered intraperitoneally in a dosage of 10 mg/kg to establish the SA-AKI model. The control group was administered the corresponding amount of 0.9% sodium chloride solution. 24 hours post-intraperitoneal injection, all mice were anesthetized with a dose of 50 mg/kg of 1% pentobarbital sodium administered intraperitoneally. Once the mice lost their nociceptive withdrawal reflex, indicating a state of deep anesthesia, blood samples were collected via ocular bleeding. Subsequently, the mice were euthanized through cervical dislocation to procure renal tissue samples for further experimentation. To ensure objectivity, the experimental procedures, as well as data collection and analysis, were rigorously conducted under double-blind conditions, thereby minimizing the influence of subjective bias on the experimental outcomes.

Renal function assessment

After allowing the blood samples to clot, they were spun at 3000 revolutions per minute for a duration of 10 minutes using a centrifuge. The collected supernatant serum underwent measurements for Scr and blood urea nitrogen (BUN) levels using an automated biochemical analyzer (ROCHE Cobas8000, Switzerland), in order to evaluate renal function.

Table 1 Primer sequence list

Genes	Forward	Reverse
GBP2	5′-TTGAGAAGGGTGACAACCAGAA-3′	5′-TGGTTCCTATGCTGTTGTAGATGAA-3′
PSMB8	5′-ATGGCGTTACTGGATCTGTGC-3′	5′-GCGGAGAAACTGTAGTGTCCC-3′
PSMB9	5′-CGTGAGGACTTTGTTAGCGCA-3	5′-CTCACATTGGTCCCAGCCA-3′
GAPDH	5′-CCTCGTCCCGTAGACAAAATG-3′	5′-TGAGGTCAATGAAGGGGTCGT-3′

Histopathology and immunohistochemistry

The mouse kidney tissue, after being fixed and dehydrated, was meticulously sectioned into thin slices. After deparaffinization, hydration, and hematoxylin-eosin (HE) staining, renal morphology was observed under an Olympus optical microscope, and tissue damage was scored based on the percentage of damaged tubules (on a scale of 0–4). For immunohistochemical analysis, the sections were first deparaffinized, hydrated, and underwent antigen retrieval. Subsequently, they were blocked using 5% goat serum. Specific antibodies for GBP2 (1:400), PSMB8 (1:200), and PSMB9 (1:400) (Proteintech, Wuhan, China) were incubated overnight at 4 °C, after PBS washing, add HRP secondary antibody, DAB staining, and finally take photos under the microscope.

RNA isolation and RT-qPCR

Total RNA was extracted from mouse renal tissues using Trizol reagent (Servicebio, Wuhan, China). After measuring RNA concentrations with a UV spectrophotometer, reverse transcription was performed to synthesize complementary DNA (cDNA) using a First Strand cDNA Synthesis Kit (Servicebio, Wuhan, China). Then the amplification process was subsequently carried out using SYBR Green qPCR Master Mix (Servicebio, Wuhan, China). Using *GAPDH* as the internal control, relative expression levels of *GBP2, PSMB8,* and *PSMB9* were derived by applying the $2^{-\Delta\Delta CT}$ method. The primer sequences used in this experiment are listed in Table 1.

Western blot analysis

Mouse kidney proteins were extracted, quantified, separated, and transferred to PVDF membranes. After being treated with a blocking agent to prevent nonspecific binding, the membranes were placed in a solution containing the primary antibodies GBP2 (1:1000), PSMB (1:1000), and PSMB9 (1:1000) (sourced from Proteintech, Wuhan, China), and incubated overnight at a low temperature (such as 4 °C). Following this, they were incubated with secondary antibodies. Chemiluminescence was detected and images were captured. The relative expression levels of GBP2, PSMB, and PSMB9 were calculated based on their comparison to β-actin.

Statistical analysis

The statistical evaluations and figure production were conducted with R software and GraphPad Prism. The levels of statistical significance were set at $p < 0.05$ denoted by *, $p < 0.01$ denoted by **, and $p < 0.001$ denoted by ***.

Results

Identification of DEGs

In the GSE240304 dataset, we selected 5 normal control samples and 5 LPS-AKI kidney tissue samples. After normalizing the gene chip data using the normalizeBetweenArrays method, the resulting boxplot (Fig, 2A) indicated a uniform data distribution, suitable for subsequent analysis. Ultimately, we identified a total of 4,782 DEGs related to LPS-AKI (details in Supplementary Table S1), with 2,238 genes showing upregulation and 2,544 genes showing downregulation in LPS-AKI kidney tissue (Fig. 2B). Additionally, a heatmap was generated to illustrate the expression patterns of the top 50 identified DEGs (Fig. 2C).

WGCNA analysis

We utilized the GSE240304 gene expression profile data to perform WGCNA analysis, aiming to identify the gene module that has the strongest association with SA-AKI. First, we rigorously screened all candidate genes and samples to ensure the absence of outliers (Fig. 3A). With a soft threshold set at 5, the scale-free network and connectivity exhibited optimal compatibility (Fig. 3B). Subsequently, we constructed a gene hierarchical clustering dendrogram by assessing the correlations between genes, identifying 20 distinct gene modules (Fig. 3C). Analyzing the clustering of module characteristic vectors clarified their interrelations (Fig. 3D). Furthermore, we explored the associations between these 20 modules and clinical symptoms (Fig. 3E). Of all these modules, the yellow module showed the strongest link to SA-AKI, marked by a correlation coefficient of 0.88 (statistically significant at $p < 0.001$), encompassing 6,293 genes in total. To visualize the relationship between gene significance within this module, we produced a scatter plot and found a notable positive correlation between GS and MM, with a correlation coefficient of 0.64 ($p < 0.001$). By setting thresholds of 0.9 for both axes, we identified 340 genes located in the top right quadrant of the scatter plot, which are considered highly associated with SA-AKI (Fig. 3F).

Functional enrichment analysis of SA-AKI characteristic genes

By cross-referencing the 340 genes identified through WGCNA with the 4,782 DEGs, we obtained 268 characteristic genes related to SA-AKI (Fig. 4A). To delve deeper into the roles and biological functions of these genes in the pathology of SA-AKI, we performed a comprehensive functional enrichment analysis. According to the GO enrichment analysis, these signature genes

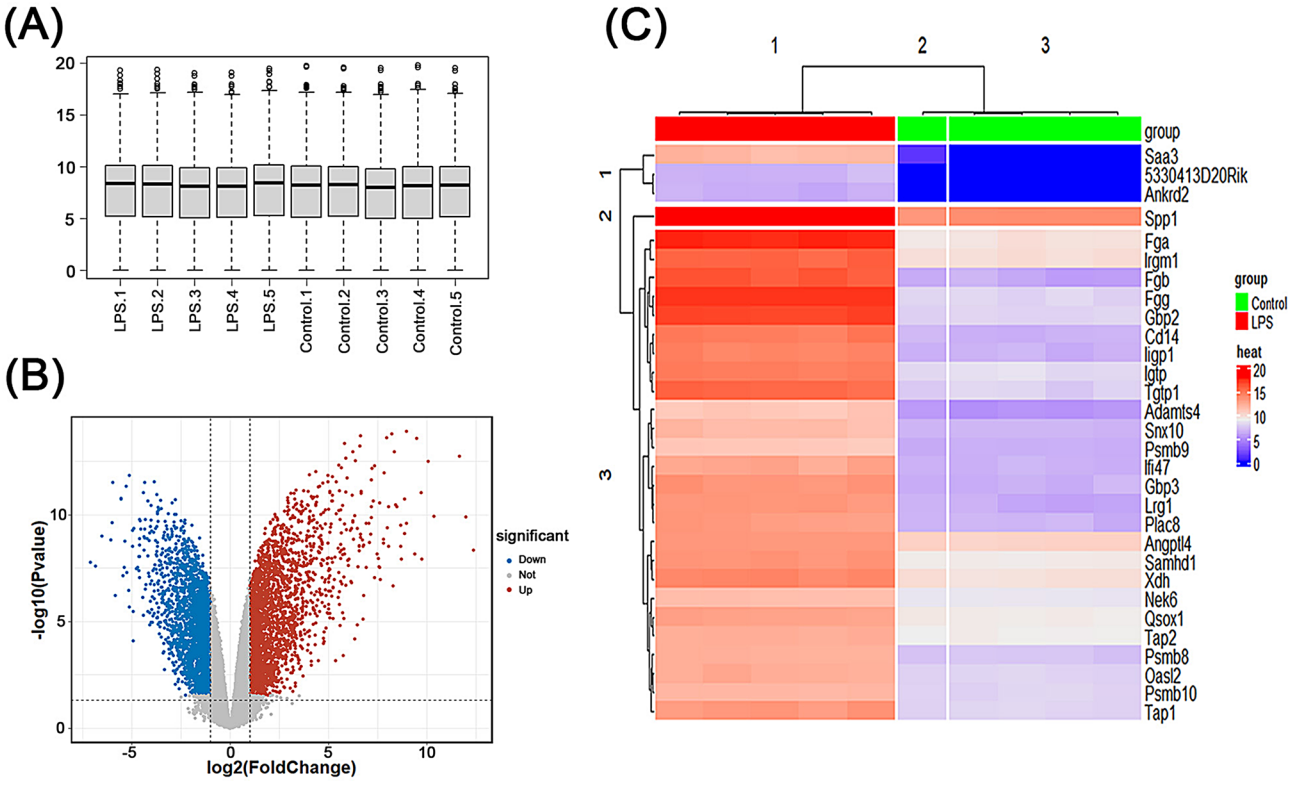

Fig. 2 Data normalization and differential expression gene screening. **(A)** Box plot illustrating data normalization: the data distribution is orderly after background adjustment and normalization. **(B)** Volcano plot showing the expression of differentially expressed genes (DEGs) between the LPS-AKI group and normal controls. **(C)** Heatmap illustrating the top 50 differentially expressed genes in the LPS-AKI group and normal controls

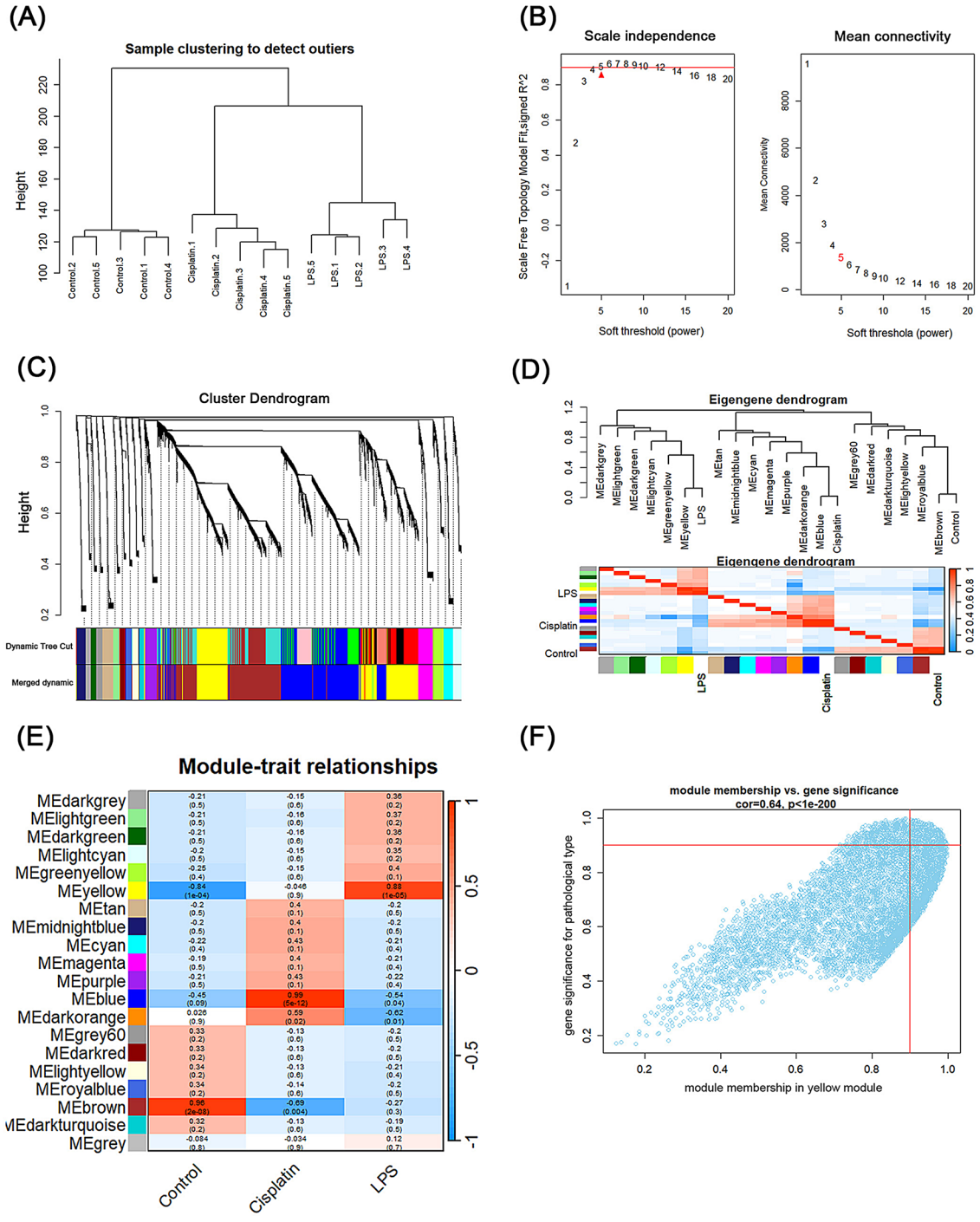

Fig. 3 Key module identification based on WGCNA. **(A)** Identification of outlier samples in GSE24030. **(B)** Scale-free fit index analysis and average connectivity for soft-thresholding power from 1 to 20. **(C)** Dendrogram of the WGCNA network, with each color representing a different module. **(D)** Correlation heatmap of module feature vector. **(E)** Heatmap showing the correlation between module and clinical characteristics. **(F)** Scatter plot of gene significance (GS) versus module membership (MM) in the yellow module

are predominantly involved in crucial BP including innate immune reactions, cellular responses to interferon, inflammatory reactions, and reactions to lipopolysaccharide. In terms of MF, they predominantly exhibit protein binding, protein homodimer activity, and GTPase activity. Regarding CC, these genes are primarily localized to the cytosolic region (Fig. 4B). KEGG pathway analysis further revealed significant enrichment of these core genes in several pathways, including the NOD-like receptor signaling pathway, chemokine

Fig. 4 Characteristic genes screening and enrichment analysis related to SA-AKI. **(A)** Venn diagram showing the intersection of DEGs and WGCNA. **(B)** Bar chart of GO enrichment analysis, including Biological Process (BP), Cellular Component (CC), and Molecular Function (MF). **(C)** Bubble chart of KEGG pathway enrichment analysis. **(D)** Chord diagram showing the relationship between signaling pathways and target genes

signaling pathway, C-type lect receptor signaling pathway, insulin signaling pathway, and Toll-like receptor signaling pathway (Fig. 4C). Additionally, we conducted an in-depth association analysis between the major signaling pathways and their corresponding target genes (Fig. 4D) (details in Supplementary Table S2). Overall, the results from the functional enrichment analysis provide strong evidence that biological processes and signaling mechanisms involved in infection, inflammation,

and innate immunity hold paramount importance in the pathological mechanisms of SA-AKI.

Identification of hub genes and evaluation of diagnostic effects

We constructed the PPI network after removing proteins that did not participate in interactions from the STRING database (Fig. 5). Using two topological algorithms, Degree and MCC, within Cytoscape software, we identified the top 15 important nodes in the PPI network (Fig. 6A, B). Concurrently, we utilized the partial likelihood deviance plot (Fig. 6C) and coefficient profiles (Fig. 6D) from LASSO regression analysis to identify 14 candidate genes. By intersecting these datasets, we ultimately recognized 3 hub genes: *GBP2, PSMB8*, and *PSMB9* (Fig. 6E).

To validate the reliability of the transcriptional activity of these core genes and their diagnostic accuracy, we selected GSE30718 as an external validation dataset. The data revealed that the levels of gene expression for *GBP2, PSMB8*, and *PSMB9* in the AKI group showed a statistically significant increase over the control group (Fig. 6F). Moreover, ROC analysis affirmed the diagnostic accuracy of these critical genes in predicting SA-AKI, with respective AUC values being 0.8233, 0.7669, and 0.6955 (Fig. 6G). These findings indicate that the identified hub

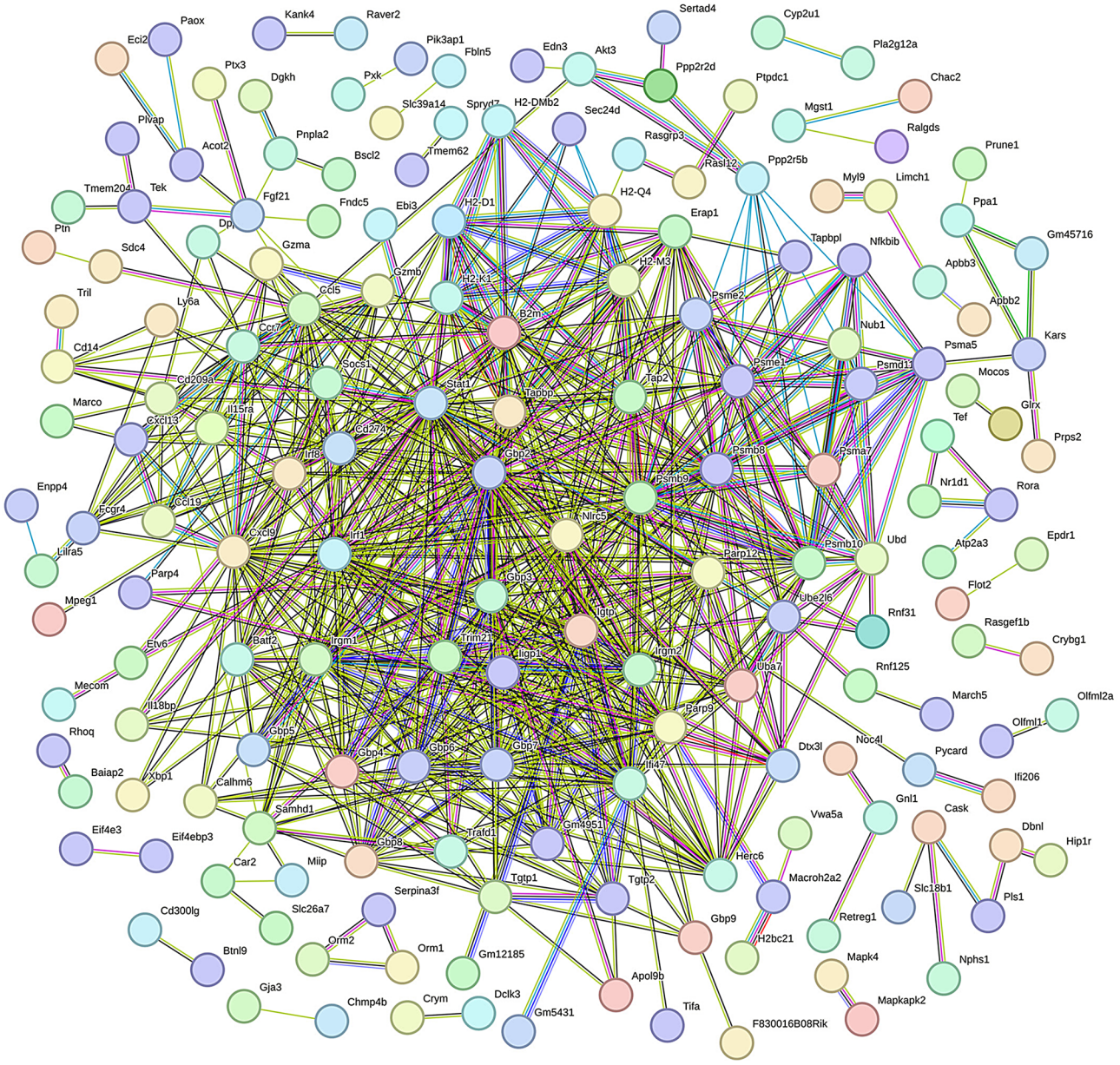

Fig. 5 PPI network diagram of characteristic genes

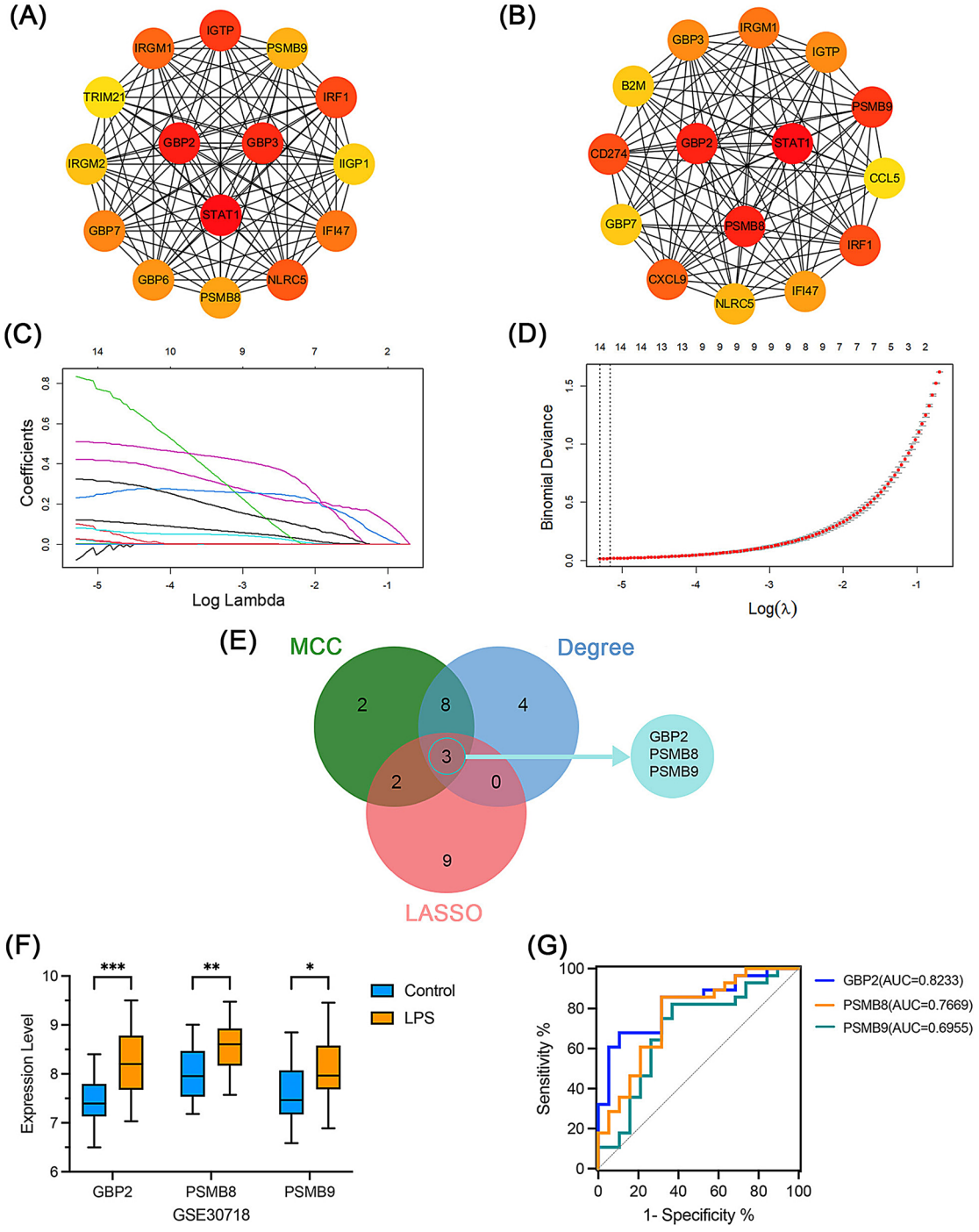

Fig. 6 Hub gene screening and diagnostic effect assessment for SA-AKI. **(A)** Top 15 hub genes in PPI ranked by maximum clique centrality (MCC). Gene colors indicate MCC scores, with darker colors representing higher scores. **(B)** Identification of top 15 hub genes in the PPI network using degree algorithm. **(C)** Variance features of the coefficients in LASSO regression analysis. **(D)** Cross-validation plot for selecting the optimal lambda value. **(E)** Venn diagram displaying the core genes shared among MCC, Degree, and LASSO. **(F)** Expression of hub genes in human kidney tissue based on GSE30718 (* $p < 0.05$, ** $p < 0.01$, *** $p < 0.001$). **(G)** ROC curve for hub genes

genes possess good diagnostic efficacy in predicting SA-AKI.

Evaluation of disease specificity for hub genes

To validate the disease specificity of the selected hub genes, we obtained multiple datasets from the GEO database concerning mouse kidney tissue, specifically the IRI-AKI dataset (GSE268009), Cis-AKI dataset (GSE106993), and CI-AKI dataset (GSE130795). Figures 7A, C demonstrate that the expression patterns of these three hub genes across these three datasets do not exhibit statistically significant differences. This finding further corroborates the effectiveness of these hub genes in distinguishing LPS-AKI from other types of AKI, such as IRI-AKI, Cis-AKI, and CI-AKI. Therefore, we tentatively conclude that these three signature genes may possess specificity for LPS-induced SA-AKI.

Furthermore, to delve deeper into the potential impact of varying infection severities on the expression levels of these three core genes, we additionally downloaded two more datasets: one for AKI induced by low-dose LPS (GSE199598) and another for AKI induced by high-dose LPS (GSE30576). As illustrated in Fig. 7D–E, under conditions of different LPS doses, the expression levels of these three hub genes exhibit statistically significant differences. Notably, within the GSE30576 dataset, we observed an intriguing phenomenon: as renal function recovered following AKI, the expression levels of these

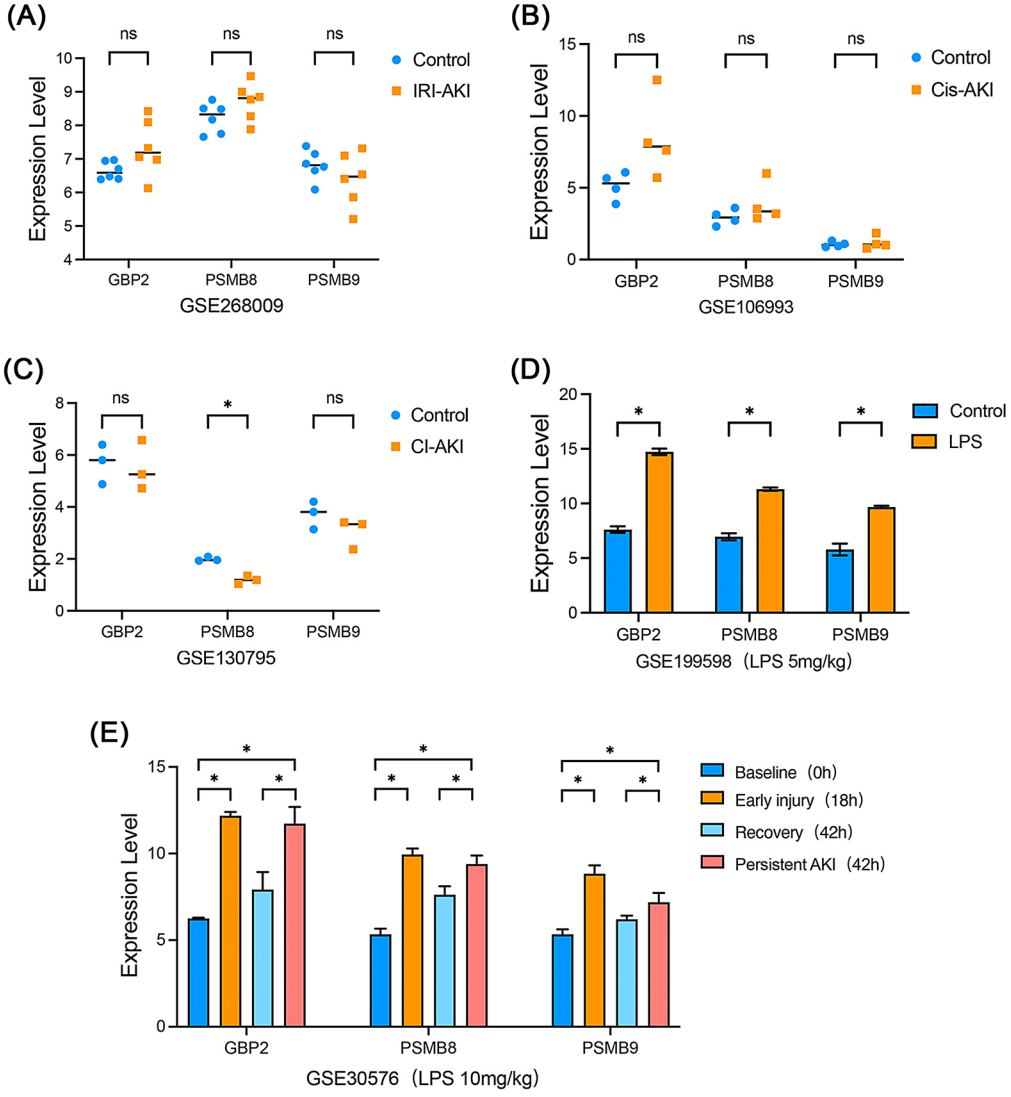

Fig. 7 The expression of hub genes in other datasets. **(A-C)** The expression profiles of three hub genes are presented across three datasets: IRI-AKI (GSE268009), Cis-AKI (GSE106993), and CI-AKI (GSE130795). **(D)** Within the LPS-AKI dataset (GSE199598), the expression levels of these three hub genes are shown for the LPS-AKI group, which received a dose of 5 mg/kg of LPS. **(E)** Following the administration of 10 mg/kg of LPS to mice, the expression of the three hub genes was assessed at various time points (0 h, 18 h, and 42 h). At the 42 h time point, the mice were further categorized into two groups: those with renal function recovery and those with persistent renal injury. (* $p < 0.05$, ns represents no significance)

three genes decreased accordingly. This discovery further suggests a possible correlation between the expression levels of these genes and the degree of kidney damage.

Immune cell infiltration analysis

We utilized the CIBERSORT algorithm to calculate the fractions of different immune cell types in each sample. Figure 8A displays the percentage distribution of various immune cells in the samples, with CD4 naive T cells being the most prevalent. The violin plot in Fig. 8B demonstrates the differences in immune cell infiltration between the two groups of samples. The research results indicate that there are significant differences ($p < 0.05$) in the percentages of nine immune cell subsets between the LPS-AKI group and the control group. Notably, there is a significant increase in neutrophils, memory B cells, M1 macrophages, activated NK cells, and activated dendritic cells, while mast cells, plasma cells, CD4 memory T cells, and resting NK cells are significantly decreased.

Furthermore, we performed a Spearman correlation analysis to investigate the relationship between the abundance of immune cells and the patterns of three core genes: *GBP2, PSMB8*, and *PSMB9*. The detailed results are shown in Fig. 8C. Specifically, *GBP2* overexpression was closely linked to the infiltration of activated dendritic cells and M1 macrophages (Fig. 8D, E). *PSMB8* expression demonstrated a strong positive association with the presence of memory B cells (Fig. 8F). By contrast, *PSMB9* expression exhibited a positive association with neutrophils(Fig. 8G) while exhibiting a negative association with plasma cells and CD4 memory T cells (Fig. 8H, I). The results indicate that these immune cell types could be modulated by the hub genes, occupying a central position in the onset and progression of SA-AKI.

Relationship between hub genes and clinical-pathological characteristics

Using the Nephroseq database, we further investigated the correlation between the mRNA expression levels of hub genes and clinical-pathological indicators. The outcomes exhibited an inverse link between the expression levels of *GBP2, PSMB8, PSMB9* and GFR, with correlation coefficients of -0.6702, -0.6283, and -0.6232 for each gene, respectively (Fig. 9A). Furthermore, the expression levels of these genes exhibited a positive linkage with Scr levels, with respective correlation coefficients of 0.6206, 0.5268, and 0.5573, all showing p-values less than 0.001 (Fig. 9B). We also compared the levels of gene expression for these genes in kidney tissues with and without proteinuria, revealing significantly elevated levels in the presence of proteinuria (Fig. 9C).

Experimental validation in the LPS-AKI mouse model

LPS-AKI mice exhibited significant increases in Scr and BUN levels within 24 hours compared to the control group (Fig. 10A, B), indicating substantial renal impairment due to LPS treatment. Histopathological examination via HE staining revealed notable vacuolar degeneration, renal tubular dilation, and necrosis of renal tubular epithelial cells in the kidney tissues of the experimental group (Fig. 10C, D), confirming the severity of renal injury.

To confirm the expression levels of the key genes—*GBP2, PSMB8*, and *PSMB9*—in the context of SA-AKI, we employed RT-qPCR (Fig. 10E-G), Western blot (Fig. 10H, I), and immunohistochemical analysis (Fig. 10J) to assess the transcriptional and translational abundance of these genes. Our findings showed a marked increase in the expression of all three hub genes in the LPS-AKI group, aligning with our previous bioinformatics predictions. This finding reinforces the critical roles of GBP2, PSMB8, and PSMB9 in the pathology of SA-AKI, offering convincing experimental proof that deepens our insight into its underlying disease mechanisms and identifies potential treatment options.

Discussion

Sepsis can trigger an imbalance in inflammatory responses and immune regulation, leading to systemic inflammatory response syndrome. The kidneys are particularly susceptible during sepsis, making AKI a common complication [25]. The primary pathological changes in SA-AKI are recognized as inflammation, microcirculatory dysfunction, and metabolic reprogramming of cells [26]. However, the exact mechanisms underlying SA-AKI remain poorly understood. During our investigation, we utilized datasets from the GEO database and employed a variety of bioinformatics methods—including DEGs, LASSO regression, WGCNA, and PPI network analysis—to comprehensively analyze the pathological processes, characteristic expression genes, and immune cell infiltration associated with SA-AKI. Our findings were further validated through external datasets and animal experiments, laying a solid scientific foundation for future investigations into SA-AKI.

Initially, we conducted WGCNA and differential expression analysis on the GSE240304 dataset, successfully identifying 268 characteristic genes significantly associated with the clinical traits of SA-AKI. In order to further explore the biological functions of these genes in the progression of the disease, we performed GO and KEGG enrichment analysis on them. The findings indicated that these genes were predominantly concentrated in biological processes and signaling cascades linked to infection, inflammation, and immunity. Key areas of enrichment included responses to interferons, innate

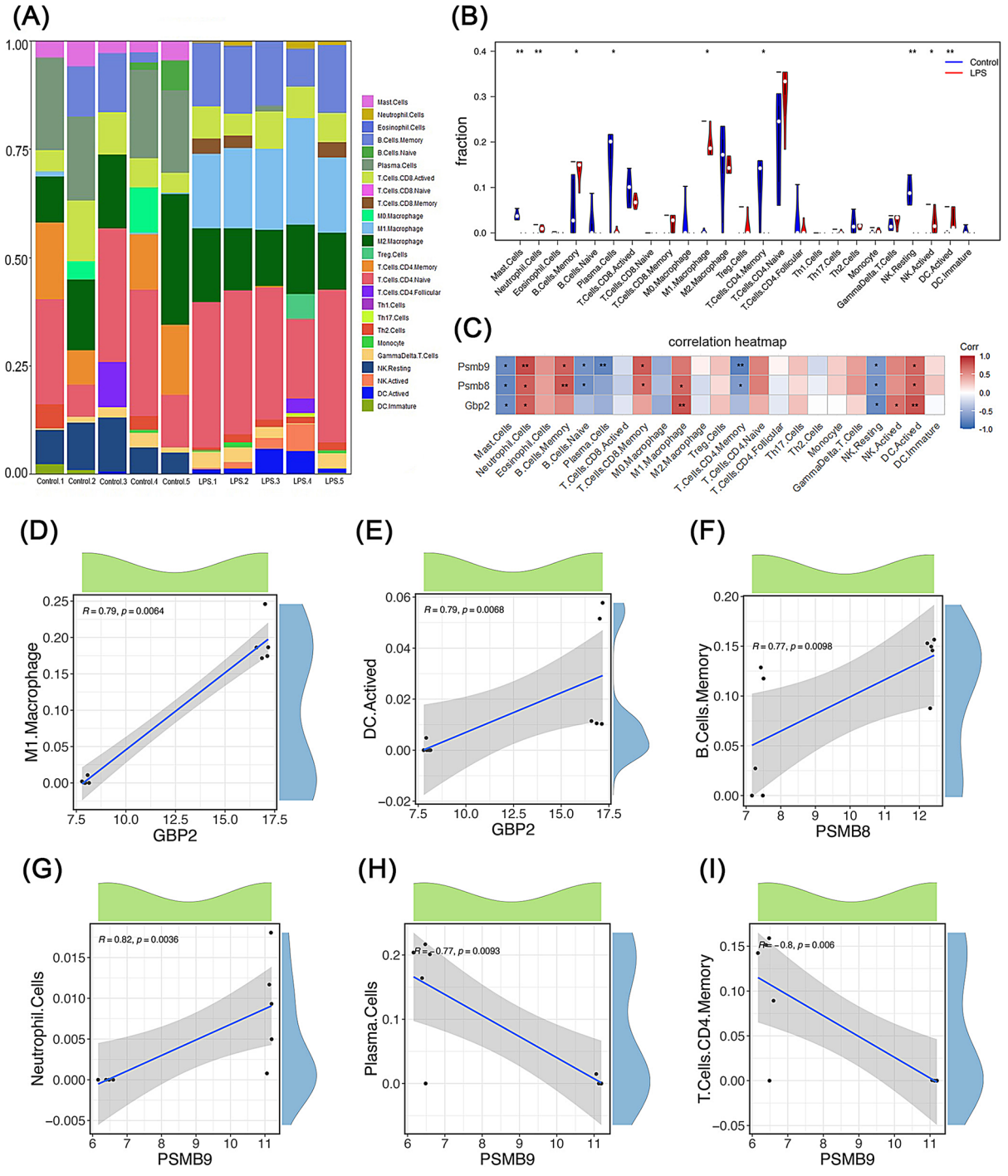

Fig. 8 Immune cell infiltration analysis in SA-AKI. **(A)** Proportions of different immune cells in each sample, with each color representing a type of immune cell. **(B)** Expression abundance of different immune cells in SA-AKI and controls (* $p < 0.05$, ** $p < 0.01$). **(C)** Correlation study between immune cells and the three core genes. Colors in the framework represent Spearman correlation coefficients between different immune cells and the three core genes (* $p < 0.05$, ** $p < 0.01$). **(D-I)** Spearman correlation analysis showing the relationships between hub genes and different immune cells

immune responses, GTPase activity, responses to LPS, antigen processing and presentation, NOD-like receptor signaling pathways, C-type lectin receptor signaling pathways, and chemokine signaling pathways.

Given that most sepsis cases arise from bacterial infections [27], innate immunity serves as a critical first line of defense. LPS, an endotoxin from Gram-negative bacteria, rapidly activates innate immune responses by promoting interferon-γ (IFN-γ) production in natural killer T cells,

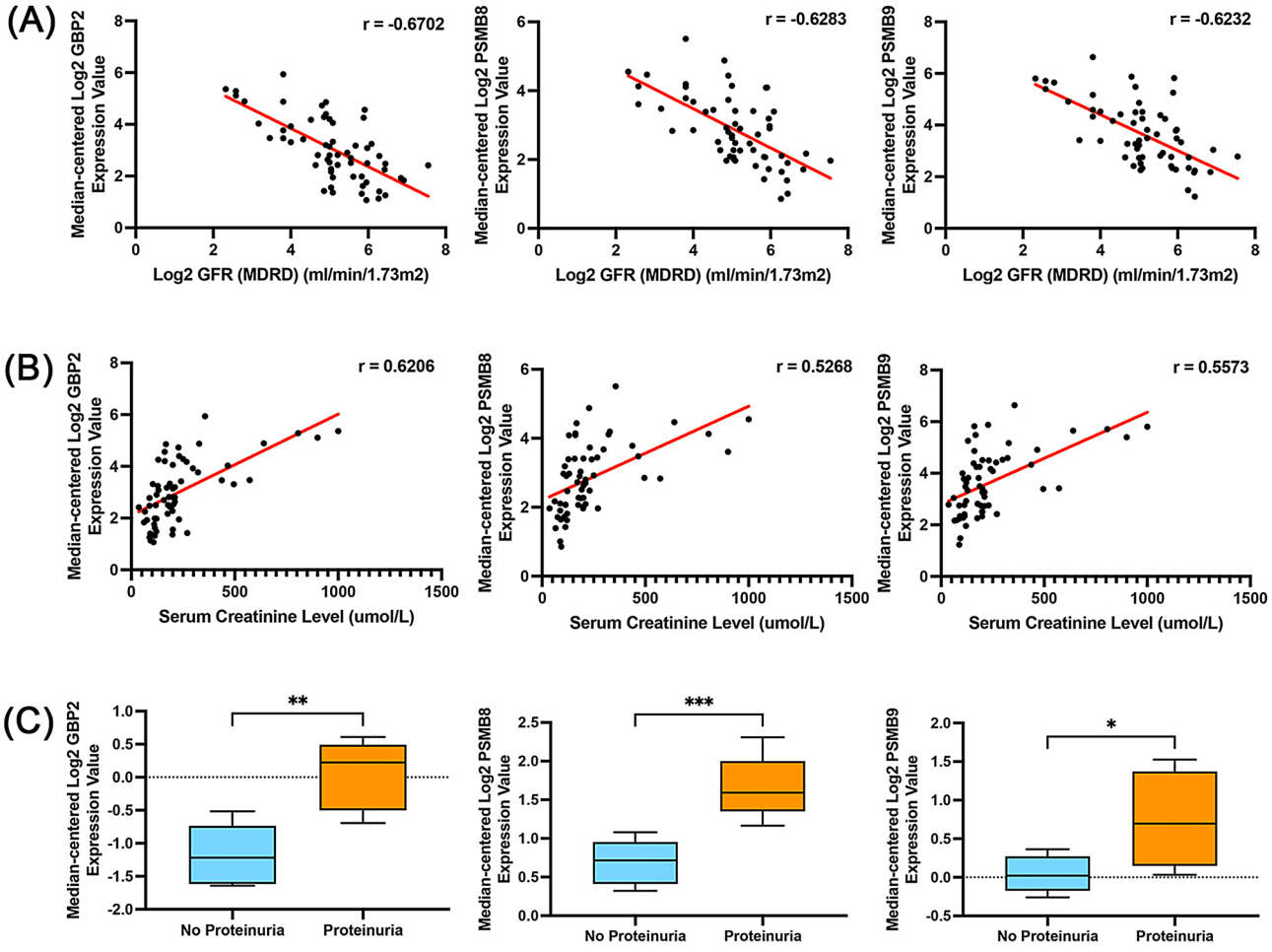

Fig. 9 Clinical-pathological correlation analysis of the three core genes. **(A)** Scatter plot showing the correlation between GBP2 (left), PSMB8 (middle), PSMB9 (right), and glomerular filtration rate. **(B)** Scatter plot showing the correlation between GBP2 (left), PSMB8 (middle), PSMB9 (right), and serum creatinine. **(C)** Box plot showing the expression differences of GBP2 (left), PSMB8 (middle), PSMB9 (right) between patients with and without proteinuria (* $p < 0.05$, ** $p < 0.01$)

which directly eliminate pathogens [28]. Additionally, AKI is closely linked to both renal and systemic inflammation. While inflammatory responses are essential for pathogen clearance and tissue repair post-injury, excessive and unresolved inflammation can lead to autoimmune diseases, fibrosis, and further tissue damage [29]. In the context of SA-AKI, bacterial infections induce dysregulated hyperactive innate immune responses, triggering a cascade of pro-inflammatory molecules that stimulate the complement system and innate immune cells, ultimately exacerbating SA-AKI [30]. In summary, previous immunological findings on the pathological mechanisms of LPS-AKI align with our enrichment analysis results, further confirming the critical roles of these signature genes in the pathology of SA-AKI.

Subsequently, to ascertain key genes within the set of characteristic genes, we built a PPI network and performed topological analyses using Cytoscape. We also employed LASSO regression analysis to further refine our selection of key hub genes. Utilizing metrics such as MCC and Degree within Cytoscape provided insights into the structure and function of the biological network, helping us identify core nodes. Ultimately, by combining dimensionality reduction and feature selection through LASSO regression, we identified three pivotal hub genes—*GBP2, PSMB8*, and *PSMB9*—that play significant roles in the development of SA-AKI.

GBP2, belonging to the guanylate-binding protein family, is an interferon-inducible protein that is prominently expressed during infections and has a pivotal function in the immune response, aiding the host in resisting pathogen invasion [31]. Research indicates that GBP2 acts as a surfactant for LPS, directly binding to it to form protein-LPS complexes that enhance caspase-4 activity [32], which is crucial for host defense against Gram-negative bacterial pathogens. Beyond its antibacterial function, GBP2 interacts with dynamin-related protein 1 (Drp1), inhibiting its translocation

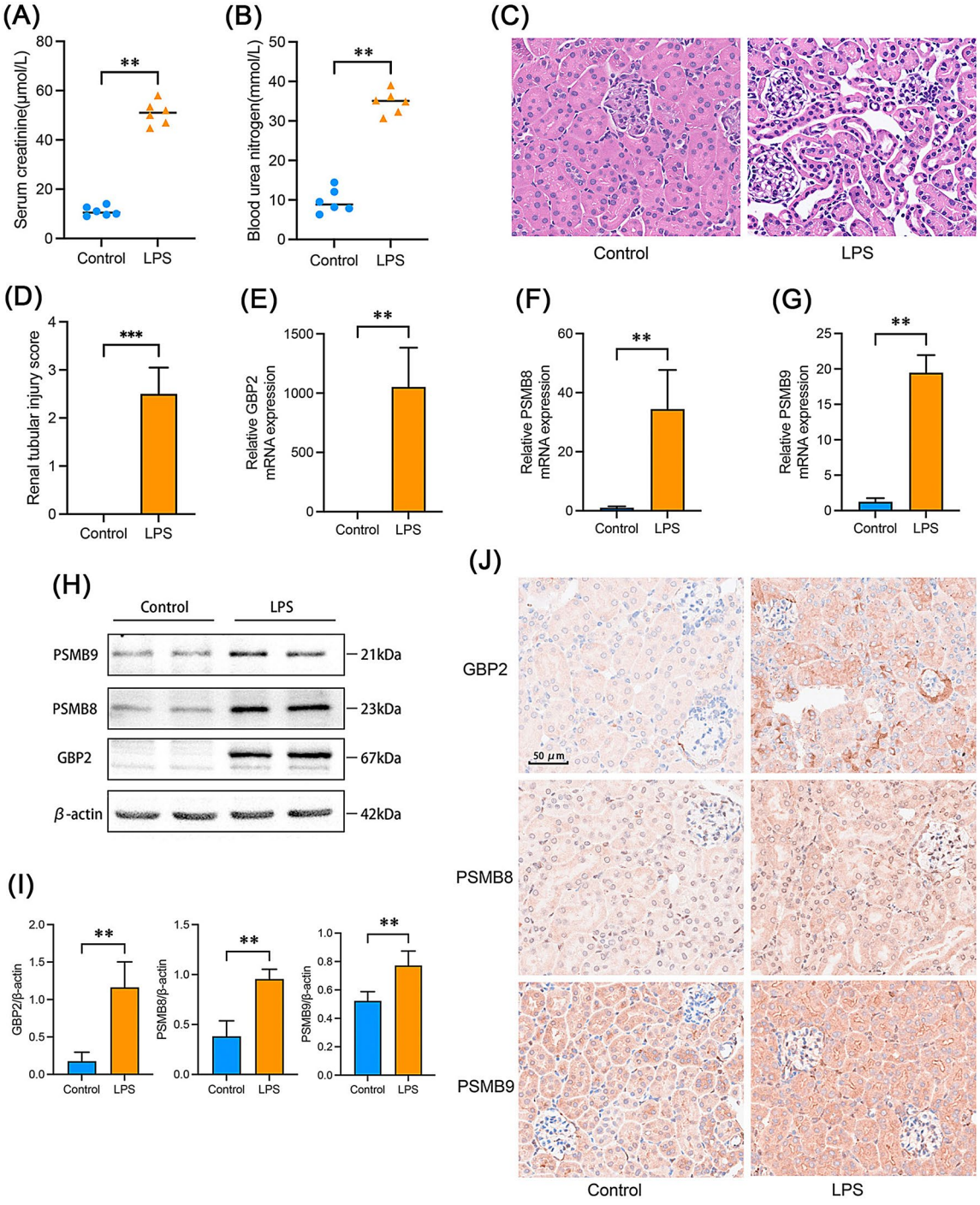

Fig. 10 Validation of the expression of three core genes in animal experiments. **(A-B)** Measurement of serum biochemical indicators in mice, including serum creatinine and blood urea nitrogen (n = 6). **(C-D)** HE staining to observe morphological changes in the kidneys and to score tubular injury (n = 6) (original magnification × 400). Scale bar = 50 micrometers. **(E-G)** Detection of mRNA levels of GBP2, PSMB8, and PSMB9 in mice using qPCR. **(H-I)** Representative Western blot images and quantification of GBP2, PSMB8, and PSMB9 expression in mouse kidney tissues. **(J)** Immunohistochemical staining of GBP2, PSMB8, and PSMB9 in mouse kidneys. Magnification: × 400, scale bar = 50 μm (* $p < 0.05$, ** $p < 0.01$)

from the cytoplasm to mitochondria [33]. This action reduces mitochondrial fission, a significant mechanism implicated in AKI, as excessive fission disrupts mitochondrial network integrity, increasing the number of smaller, more oxidative-stress-susceptible mitochondria. This ultimately leads to diminished ATP production and exacerbates the energy crisis in renal cells [34]. Thus, we hypothesize that GBP2 may also mitigate SA-AKI

through this regulatory pathway, although further experimental validation is warranted.

PSMB8 (LMP7) and PSMB9 (LMP2) are essential components of the proteasome, encoding β5i and β1i subunits with trypsin-like and caspase-like activities, respectively. The proteasome is crucial for protein degradation and cell cycle regulation in kidney diseases [35]. Studies have shown that PSMB8 and PSMB9 are involved in T cell regulation following renal tubular injury, significantly influencing inflammation progression [36]. The regulatory function of PSMB8 in inflammation may be mediated through the PERK/NF-κB signaling pathway [37]. Additionally, both genes have been identified as susceptibility loci in IgA nephropathy [38]. Further research suggests that PSMB8 and PSMB9 have substantial potential in treating inflammatory diseases, and their combined use may produce significant synergistic effects in suppressing inflammation [39]. In summary, inflammation and immune responses are crucial element in the onset and development of SA-AKI, our findings, alongside existing literature. Our results highlight the critical roles of GBP2, PSMB8, and PSMB9 in the pathology of SA-AKI, although their specific molecular mechanisms require further exploration.

We further carried out an immune cell infiltration analysis to comprehensively assess the dysregulation of immune cells in SA-AKI. The results revealed significantly elevated levels of neutrophils, activated dendritic cells, M1 macrophages, memory B cells, and activated NK cells in kidney tissues following LPS treatment. Conversely, we observed decreases in mast cells, resting NK cells, plasma cells, and CD4 + memory T cells. Furthermore, significant correlations were identified between the hub genes (*GBP2, PSMB8*, and *PSMB9*) and various major immune cells, including neutrophils, mast cells, activated dendritic cells, memory B cells, plasma cells, CD4 + memory T cells, CD8 + memory T cells, M1 macrophages, and NK cells. The results imply that these key genes may exert a significant influence on the immune regulation of SA-AKI and are strongly linked to the malfunction of inflammatory cells within this framework.

Neutrophils, vital innate immune effectors, are essential to elucidating the pathophysiology of renal injury. Upon activation, they release reactive oxygen species and various substances that induce intracellular oxidative stress and mitochondrial dysfunction, resulting in tissue damage [40]. After ischemia-reperfusion injury, neutrophils are recruited to the kidneys and become the primary effector cells in this process [41]. M1 macrophages, when stimulated by LPS and IFN-γ, release a variety of cytokines that promote inflammation, thereby facilitating the initiation and advancement of inflammatory responses [42]. Dendritic cells are pivotal members of the immune system, capable of initiating adaptive immune responses by capturing, processing, and presenting antigens to T cells. They serve as a crucial bridge linking innate immunity and adaptive immunity. Clinical trials have demonstrated that manipulating dendritic cell immune tolerance can effectively improve outcomes in AKI [43]. Memory B cells, which retain the ability to remember antigens, enable the body to mount rapid and robust immune responses upon re-exposure to pathogens. An elevated level of memory B cells has been detected in the peripheral blood of individuals with AKI resulting from Epstein-Barr virus infection [44]. Natural killer cells are also key cells of the innate immune system, capable of triggering apoptosis in tubular epithelial cells, which exacerbates renal ischemia-reperfusion injury [45]. Elevated expression of cytotoxic molecules on NK cells has been noted in patients with severe sepsis-related AKI, suggesting that inhibiting excessive NK cell activation may be a promising avenue for preventing and treating AKI [46].

In conclusion, these results emphasize the significance of inflammation and autoimmunity in the progression of SA-AKI. The insights gained from this research establish a basis for a deeper comprehension of the underlying mechanisms of SA-AKI and open avenues for exploring new treatment strategies.

Nevertheless, recognizing the constraints of our research is essential. Firstly, a small sample size could lead to potential biases in sequencing outcomes. Future studies should aim to increase the sample size for gene sequencing to minimize this bias. Second, while we identified three core genes, their specific mechanisms of action in SA-AKI remain unclear. Gene knockout models are indispensable for future exploration into the functions and regulatory dynamics of these genes. These endeavors will deepen our comprehension of SA-AKI's pathogenesis and facilitate the creation of new treatment approaches.

Conclusion

In conclusion, our research shows that immune and inflammatory reactions occupy a pivotal position in the development of SA-AKI, with the resultant inflammatory environment potentially serving as its primary pathophysiological characteristic. We identified three novel candidate genes—*GBP2, PSMB8*, and *PSMB9*—that may function as biomarkers or therapeutic targets. The expression levels of these genes have been validated at both the mRNA and protein levels in mouse models; however, their specific mechanisms of action require further exploration, which will be a crucial focus for future research.

Abbreviations

AKI	Acute kidney injury
SA-AKI	Sepsis-associated acute kidney injury

BP	Biological process
CC	Cellular component
MF	Molecular function
GEO	Gene Expression Omnibus
GO	Gene Ontology
KEGG	Kyoto Encyclopedia of Genes and Genomes
WGCNA	Weighted gene co-expression network analysis
LASSO	Least absolute shrinkage and selection operator
ROC	Receiver operating characteristic curve
AUC	Area under curve
PPI	Protein-protein interaction network
DEGs	Differentially expressed genes
LPS	Lipopolysaccharide
IRI	Ischemia-reperfusion injury
logFC	Log fold change
RT-qPCR	Real-time quantitative polymerase chain reaction
GFR	Glomerular filtration rate
Scr	Serum creatinine
MCC	Maximum clique centrality
GS	Gene significance
MM	Module membership
Cis-AKI	Cisplatin-induced acute kidney injury
CI-AKI	Contrast-induced acute kidney injury
BUN	Blood urea nitrogen

Supplementary Information

The online version contains supplementary material available at https://doi.org/10.1186/s12882-025-04069-4.

Supplementary Material 1

Supplementary Material 2

Acknowledgments
The author thanks GEO, DAVID, STRING, CIBERSORT, and Nephroseq for providing the platforms. The author is grateful all participants for their continued participation and contribution to this research project.

Authors contributions
HY: design of the study, interpretation of data, data analysis and wrote the manuscript; XZ: design of the study, interpretation of data reviewing and editing the manuscript; PL, MW and RL: explored literature. DY designed and supervised the study. All authors have read and approved the final manuscript.

Funding
This work was supported by the National Natural Science Foundation of China (No. 81670631 to Dingping Yang).

Data availability
The data that support the findings of this study are available from the corresponding author, upon reasonable request.

Declarations

Ethics approval and consent to participate
The bioinformatics analysis section of our research utilized publicly available data, did not involve human participants, and thus did not necessitate ethical considerations related to consent, confidentiality, or privacy of participants. The experimental verification involving animals received approval from the Animal Experimentation Ethics Committee at Renmin Hospital of Wuhan University (IACUC Issue NO.20211103), and adhered to the pertinent animal ethics guidelines.

Consent for publication
Not applicable.

Competing interests
The authors declare no competing interests.

Author details
[1]Department of Nephrology, Renmin Hospital of Wuhan University, Wuhan, China
[2]Department of Transfusion, Wuhan Third Hospital (Tongren Hospital of Wuhan University), Wuhan, China
[3]Nephrology and Urology Research Institute of Wuhan University, Wuhan, China
[4]Department of Clinical Laboratory, Tongji Hospital, Tongji Medical College, Huazhong University of Science and Technology, Wuhan, China

Received: 26 November 2024 / Accepted: 13 March 2025
Published online: 29 March 2025

References

1. White KC, Serpa-Neto A, Hurford R, Clement P, Laupland KB, See E, et al. Sepsis-associated acute kidney injury in the intensive care unit: incidence, patient characteristics, timing, trajectory, treatment, and associated outcomes. A multicenter, observational study. Intensive Care Med. 2023;49:1079–89.
2. Nandagopal N, Reddy PK, Ranganathan L, Ramakrishnan N, Annigeri R, Venkataraman R. Comparison of epidemiology and outcomes of acute kidney injury in critically ill patients with and without sepsis. Indian J Crit Care Med Peer-Rev Off Publ Indian Soc Crit Care Med. 2020;24:258–62.
3. Monard C, Rimmelé T, Blanc E, Goguillot M, Bénard S, Textoris J. Economic burden of in-hospital AKI: a one-year analysis of the nationwide French hospital discharge database. BMC Nephrol. 2023;24:343.
4. Manrique-Caballero CL, Del Rio-Pertuz G, Gomez H. Sepsis-associated acute kidney injury. Crit Care Clin. 2021;37:279–301.
5. De Backer D, Donadello K, Taccone FS, Ospina-Tascon G, Salgado D, Vincent J-L. Microcirculatory alterations: potential mechanisms and implications for therapy. Ann Intensive Care. 2011;1:27.
6. Jang HR, Rabb H. Immune cells in experimental acute kidney injury. Nat Rev Nephrol. 2015;11:88–101.
7. Fry DE. Sepsis, systemic inflammatory response, and multiple organ dysfunction: the mystery continues. Am Surg. 2012;78:1–8.
8. Gómez H, Kellum JA, Ronco C. Metabolic reprogramming and tolerance during sepsis-induced AKI. Nat Rev Nephrol. 2017;13:143–51.
9. Mutz K-O, Heilkenbrinker A, Lönne M, Walter J-G, Stahl F. Transcriptome analysis using next-generation sequencing. Curr Opin Biotechnol. 2013;24:22–30.
10. Tesi N, van der Lee S, Hulsman M, Holstege H, Reinders M. Bioinformatics strategies for the analysis and integration of large-scale multiomics data. J Gerontol A Biol Sci Med Sci. 2023;78:659–62.
11. Zhou L, Li H, Hu J, Meng J, Lv H, Yang F, et al. Plasma oxidative lipidomics reveals signatures for sepsis-associated acute kidney injury. Clin Chim Acta Int J Clin Chem. 2023;551:117616.
12. Zhao Q, Ma J, Xiao J, Feng Z, Liu H. Data driven analysis reveals prognostic genes and immunological targets in human sepsis-associated acute kidney injury. World J Emerg Med. 2024;15:91–97.
13. Liu B, Ao S, Tan F, Ma W, Liu H, Liang H, et al. Transcriptomic analysis and laboratory experiments reveal potential critical genes and regulatory mechanisms in sepsis-associated acute kidney injury. Ann Transl Med. 2022;10:737.
14. Li L, Ling Z, Wang X, Zhang X, Li Y, Gao G. Proteomics-based screening of AKR1B1 as a therapeutic target and validation study for sepsis-associated acute kidney injury. PeerJ. 2024;12:e16709.
15. Xu J, Li J, Li Y, Shi X, Zhu H, Chen L. Multidimensional Landscape of SA-AKI revealed by integrated proteomics and metabolomics analysis. Biomolecules. 2023;13:1329.
16. Dai X, Shen L. Advances and trends in omics technology development. Front Med. 2022;9:911861.
17. Langfelder P, Horvath S. WGCNA: an R package for weighted correlation network analysis. BMC Bioinf. 2008;9:559.
18. Pomaznoy M, Ha B, Peters B. GOnet: a tool for interactive gene ontology analysis. BMC Bioinf. 2018;19:470.
19. Kanehisa M, Furumichi M, Tanabe M, Sato Y, Morishima K. KEGG: new perspectives on genomes, pathways, diseases and drugs. Nucleic Acids Res. 2017;45:D353–61.
20. Sherman BT, Hao M, Qiu J, Jiao X, Baseler MW, Lane HC, et al. DAVID: a web server for functional enrichment analysis and functional annotation of gene lists (2021 update). Nucleic Acids Res. 2022;50:W216–21.
21. Szklarczyk D, Kirsch R, Koutrouli M, Nastou K, Mehryary F, Hachilif R, et al. The STRING database in 2023: protein-protein association networks and

functional enrichment analyses for any sequenced genome of interest. Nucleic Acids Res. 2023;51:D638–46.
22. Franz M, Lopes CT, Fong D, Kucera M, Cheung M, Siper MC, et al. Cytoscape.js 2023 update: a graph theory library for visualization and analysis. Bioinforma Oxf Engl. 2023;39:btad031.
23. Li Z, Sillanpää MJ. Overview of LASSO-related penalized regression methods for quantitative trait mapping and genomic selection. TAG Theor Appl Genet Theor Angew Genet. 2012;125:419–35.
24. Chen Z, Huang A, Sun J, Jiang T, Qin -FX-F, Wu A. Inference of immune cell composition on the expression profiles of mouse tissue. Sci Rep. 2017;7:40508.
25. Uchino S, Kellum JA, Bellomo R, Doig GS, Morimatsu H, Morgera S, et al. Acute renal failure in critically ill patients: a multinational, multicenter study. Jama. 2005;294:813–18.
26. Gómez H, Kellum JA. Sepsis-induced acute kidney injury. Curr Opin Crit Care. 2016;22:546–53.
27. O'Brien JM, Ali NA, Aberegg SK, Abraham E. Sepsis. Am J Med. 2007;120:1012–22.
28. Nagarajan NA, Kronenberg M. Invariant NKT cells amplify the innate immune response to lipopolysaccharide. J Immunol (Baltimore, MD). 2007;178:2706–13.
29. Rabb H, Griffin MD, McKay DB, Swaminathan S, Pickkers P, Rosner MH, et al. Inflammation in AKI: current understanding, key questions, and knowledge gaps. J Am Soc Nephrol JASN. 2016;27:371–79.
30. Kuwabara S, Goggins E, Okusa MD. The pathophysiology of sepsis-associated AKI. Clin J Am Soc Nephrol CJASN. 2022;17:1050–69.
31. Kirkby M, Enosi Tuipulotu D, Feng S, Lo Pilato J, Man SM. Guanylate-binding proteins: mechanisms of pattern recognition and antimicrobial functions. Trends Biochem Sci. 2023;48:883–93.
32. Dickinson MS, Kutsch M, Sistemich L, Hernandez D, Piro AS, Needham D, et al. LPS-aggregating proteins GBP1 and GBP2 are each sufficient to enhance caspase-4 activation both in cellulo and in vitro. Proc Natl Acad Sci U S A. 2023;120:e2216028120.
33. Zhang J, Zhang Y, Wu W, Wang F, Liu X, Shui G, et al. Guanylate-binding protein 2 regulates Drp1-mediated mitochondrial fission to suppress breast cancer cell invasion. Cell Death Dis. 2017;8:e3151.
34. Zhan M, Brooks C, Liu F, Sun L, Dong Z. Mitochondrial dynamics: regulatory mechanisms and emerging role in renal pathophysiology. Kidney Int. 2013;83:568–81.
35. Meyer-Schwesinger C. The ubiquitin-proteasome system in kidney physiology and disease. Nat Rev Nephrol. 2019;15:393–411.
36. Li C, Su F, Zhang L, Liu F, Fan W, Li Z, et al. Identifying potential diagnostic genes for diabetic nephropathy based on hypoxia and immune status. J Inflamm Res. 2021;14:6871–91.
37. Guo T, Liu C, Yang C, Wu J, Su P, Chen J. Immunoproteasome subunit PSMB8 regulates microglia-mediated neuroinflammation upon manganese exposure by PERK signaling. Food Chem Toxicol Int J Publ Br Ind Biol Res Assoc. 2022;163:112951.
38. Jia N-Y, Liu X-Z, Zhang Z, Zhang H. Weighted gene co-expression network analysis reveals different immunity but shared renal pathology between iga nephropathy and lupus nephritis. Front Genet. 2021;12:634171.
39. Basler M, Lindstrom MM, LaStant JJ, Bradshaw JM, Owens TD, Schmidt C, et al. Co-inhibition of immunoproteasome subunits LMP2 and LMP7 is required to block autoimmunity. EMBO Rep. 2018;19:e46512.
40. Jaeschke H. Mechanisms of Liver Injury. II. Mechanisms of neutrophil-induced liver cell injury during hepatic ischemia-reperfusion and other acute inflammatory conditions. Am J Physiol Gastrointest Liver Physiol. 2006;290:G1083–1088.
41. Ferhat M, Robin A, Giraud S, Sena S, Goujon J-M, Touchard G, et al. Endogenous IL-33 contributes to kidney ischemia-reperfusion injury as an Alarmin. J Am Soc Nephrol JASN. 2018;29:1272–88.
42. Kadomoto S, Izumi K, Mizokami A. Macrophage polarity and disease control. Int J Mol Sci. 2021;23:144.
43. N Y, I T. Tolerogenic dendritic cells: promising cell therapy for acute kidney injury. Kidney Int. 2023;104(3):420–22.
44. Acharya R, Zeng X, Upadhyay K. Concomitant nephrotic syndrome and tubulointerstitial nephritis in a child with Epstein-Barr virus mononucleosis. BMJ Case Rep. 2021;14:e240108.
45. Zhang Z-X, Wang S, Huang X, Min W-P, Sun H, Liu W, et al. NK cells induce apoptosis in tubular epithelial cells and contribute to renal ischemia-reperfusion injury. J Immunol (Baltimore, MD). 2008;181:7489–98.
46. Uchida T, Seki S, Oda T. Infections, reactions of natural killer T cells and natural killer cells, and kidney injury. Int J Mol Sci. 2022;23:479.

Publisher's Note